Int. J. Heat Mass Transfer. Vol. 24, No. 10, pp. 1621–1629, 1981
Printed in Great Britain

0017-9310/81/101621-09 $02.00/0

HIGH RAYLEIGH NUMBER CONVECTION IN SHALLOW ENCLOSURES WITH DIFFERENT END TEMPERATURES

G. SHIRALKAR†, A. GADGIL‡ and C. L. TIEN§
University of California, Berkeley, CA 94720, U.S.A.

(*Received* 4 *August* 1980 *and in revised form* 24 *March* 1981)

Abstract—Buoyancy-driven laminar convection in shallow horizontal enclosures (width/height $\gg 1$) with adiabatic horizontal walls and isothermal vertical walls of different temperatures has been investigated for very high Rayleigh numbers ($Ra \gg 10^6$). It is found that this flow regime, which is characterized by boundary layers lining both the vertical and horizontal walls, differs qualitatively from the low-Ra flow regime, in which the horizontal boundary layers are absent. The decreasing influence of Ra on the Nusselt number and the effect of the aspect ratio are analytically shown and then numerically verified. Comparison is made with existing experimental and numerical data, and a new correlation is proposed for the Nusselt number in this flow regime. An explanation is also advanced regarding the current controversy about the power dependence of the Nusselt number on Ra in narrow vertical channels.

NOMENCLATURE

A_1, dimensionless constant of integration;
a, dimensionless vertical temperature gradient;
B, width to height aspect ratio, L/H;
C, dimensionless characteristic velocity;
d, defined by $Nu = dRa^p$;
g, gravitational acceleration [m/s^2];
H, enclosure height [m];
L, enclosure width [m];
m, local power dependence of Nu on Ra;
$\dot{m}$, dimensionless flow rate in the horizontal boundary layer;
Nu, Nusselt number based on height;
Nu_∞, asymptotic value of Nu as $Ra \to \infty$;
n, local power dependence of Nu on B;
p, defined by $Nu = dRa^p$;
Pr, Prandtl number;
q, local power dependence of boundary layer thickness on B;
r, local power dependence of **a** on B;
Ra, Rayleigh number based on height H and ΔT;
T, temperature [K];
T_c, cold wall temperature [K];
T_H, hot wall temperature [K];
ΔT, temperature differential across enclosure, $(T_H - T_c)$;
u^*, horizontal velocity [m/s];
u, dimensionless horizontal velocity, u^*H/α;
v^*, vertical velocity [m/s];
v, dimensionless vertical velocity, v^*H/α;
X, horizontal Cartesian coordinate [m], Fig. 1;
x, dimensionless horizontal coordinate, X/H;
Y, vertical Cartesian coordinate [m], Fig. 1;
y, dimensionless vertical coordinate, Y/H.

Greek symbols

α, fluid thermal diffusivity [m^2/s];
δ, dimensionless boundary layer thickness;
ψ^*, stream function [m^2/s];
ψ, dimensionless stream function, ψ^*/α;
θ, dimensionless temperature, $(T - T_c)/(T_H - T_c)$;
ω, dimensionless vorticity, $(\partial v/\partial x - \partial u/\partial y)$.

Subscripts

b, bottom wall;
t, top wall.

1. INTRODUCTION

LAMINAR free convection in shallow horizontal enclosures (width/height $\gg 1$) bounded by adiabatic horizontal walls and isothermal end walls at different temperatures was first investigated by Cormack, Leal and Imberger [1]. Their theory for asymptotically long enclosures was extended to the high Rayleigh number range by Bejan and Tien [2] who developed an approximate solution by matching a boundary layer solution in the end region with the solution for the fully developed flow in the central 'core' of the enclosure as predicted by Cormack, Leal and Imberger. For a given large Rayleigh number, such a fully-developed inertia-free flow will exist in the core for sufficiently large B, the enclosure's width-to-height aspect ratio. For smaller widths, however, the flow is qualitatively different in the core. Experiments by Al-Homoud and Bejan [3], performed with water at $B = 16$ and $Ra \geqslant 10^8$, clearly indicate that under such conditions the core is largely stagnant except for boundary layers lining the top and bottom walls through which most of the heat transfer occurs.

† Graduate Research Assistant in Mechanical Engineering.
‡ Staff Scientist, Passive Solar Analysis and Design Group, Lawrence Berkeley Laboratory.
§ Professor of Mechanical Engineering.

The problem considered here is that of buoyancy induced laminar flow in an enclosure with a large but finite B for the case of $Ra \to \infty$. This flow regime has received scant attention in the literature. A simple analytical model which captures the essential physics of this regime is established on the basis of the experimental evidence and numerical simulation. A qualitative solution is obtained for the core as a first approximation, and matched with the end-region solution obtained earlier by Bejan and Tien [2]. This yields the functional dependence of the Nusselt number on the Rayleigh number in the form $Nu = dRa^p$, where the coefficient d is a function of the Prandtl number and the aspect ratio B. It is shown that the previous work by Gill [4] for moderate aspect ratios leads to a Ra dependence ($Nu \sim Ra^{1/4}$) which is only asymptotically valid as $Ra \to \infty$, for shallow enclosures. Finally, numerical results are presented for $Pr = 1$ and $B = 5$ and 10 which strongly support the assumptions and results of the analytical model. Correlations for the heat transfer are then proposed on the basis of the analytical and numerical results.

2. GOVERNING EQUATIONS

The geometry of the enclosure is shown in Fig. 1. The enclosure has isothermal vertical walls, one hot and one cold. The horizontal walls are insulated. For steady, laminar 2-D flow the governing equations are:

$$\frac{1}{Pr}\left(u\frac{\partial\omega}{\partial x} + v\frac{\partial\omega}{\partial y}\right) = \frac{\partial^2\omega}{\partial x^2} + \frac{\partial^2\omega}{\partial y^2} + Ra\frac{\partial\theta}{\partial x} \quad (1)$$

$$u\frac{\partial\theta}{\partial x} + v\frac{\partial\theta}{\partial y} = \frac{\partial^2\theta}{\partial x^2} + \frac{\partial^2\theta}{\partial y^2} \quad (2)$$

$$\frac{\partial^2\psi}{\partial x^2} + \frac{\partial^2\psi}{\partial y^2} = -\omega \quad (3)$$

$$u = \partial\psi/\partial y, \quad v = -\partial\psi/\partial x. \quad (4)$$

Here, the Boussinesq approximation has been used. The boundary conditions are:

$$\begin{aligned} &\text{at } x = 0: && \theta = 0, && u = v = \psi = 0, \\ &\text{at } x = B: && \theta = 1, && u = v = \psi = 0, \\ &\text{at } y = 0, 1: && \partial\theta/\partial y = 0, && u = v = \psi = 0. \end{aligned} \quad (5)$$

The Nusselt number is given by:

$$Nu = \int_0^1 (\partial\theta/\partial x - u\theta)\,dy = \int_0^1 (\partial\theta/\partial x)_{x=0}\,dy. \quad (6)$$

Clearly, Nu depends on Ra, Pr and B. The problem addressed here is to estimate the effect of Ra in the boundary layer regime for the case of large but finite B and for moderately high Prandtl numbers. It is noted that the $Pr \to 0$ case is qualitatively different from the one considered here, although both imply a deviation from the case of the inertia-free fully-developed flow in the core.

3. CORE REGION ANALYSIS

At large but finite values of B, a continuous increase of Ra will lead from a flow of the type considered by Bejan and Tien [2] to a flow which is qualitatively different, and one which is evident from the experiments of Al-Homoud and Bejan [3]. This flow is characterized by fast moving boundary layers lining the horizontal walls, through which most of the heat transfer takes place.

Near the mid-height in the core ($y = 0.5$) the fluid is observed to be stagnant [3], in consistency with zero buoyancy. Numerical solution to the full equations of motion to be presented later also show that the isotherms and streamlines are indeed very close to horizontal and $u \simeq 0$ and $v \simeq 0$ near $y \simeq 0.5$ throughout the core. The applicable equations in this region then are:

$$u = 0, \quad v = 0, \quad Ra\,(\partial\theta/\partial x) = 0, \quad (7)$$

$$\partial^2\theta/\partial y^2 = 0. \quad (8)$$

At $y = 0.5$, $\theta = 0.5$ (based on experimental observation) so that the solution to equation (8) is:

$$\theta(y) = \mathbf{a}(y - 0.5) + 0.5, \quad (9)$$

where $\mathbf{a}$ is relatively independent of x. Thus, we have a picture, consistent with experiment, of vertical conduction in the core between the two boundary layers moving in opposite directions.

The experiments also indicate, as pointed out by the authors [3], that the flow in the core is not driven by local buoyancy but rather by the momentum imparted by the vertical boundary layers in the end region. Accordingly, the applicable equations in the boundary layers lining the horizontal surfaces are, using standard boundary layer arguments:

$$\frac{1}{Pr}\left(u\frac{\partial\omega}{\partial x} + v\frac{\partial\omega}{\partial y}\right) = \frac{\partial^2\omega}{\partial y^2} + Ra\frac{\partial\theta}{\partial x} \quad (10)$$

$$\partial^2\theta/\partial y^2 = 0. \quad (11)$$

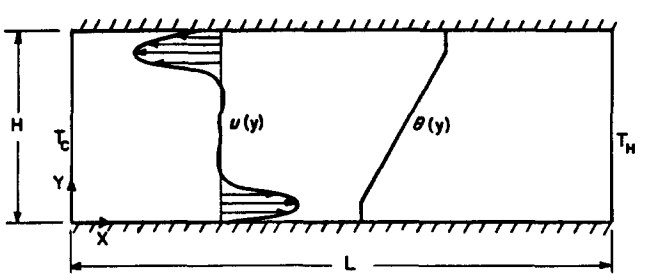

FIG. 1. Enclosure geometry.

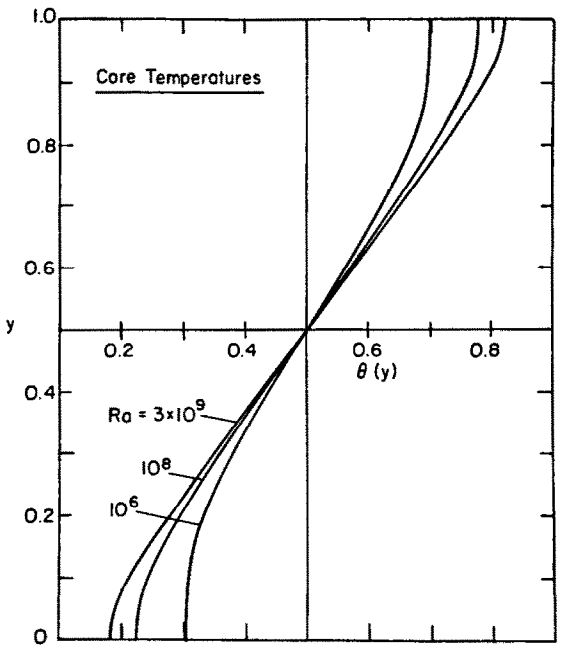

FIG. 2. Computed temperature profiles in the core, $B = 5$, $Pr = 1$.

The boundary conditions for the lower horizontal boundary layer, of thickness δ, are:

$$\text{At } y = 0, \qquad u = 0 \text{ and } \partial\theta/\partial y = 0 \tag{12}$$

$$\text{At } y/\delta \to \infty, \qquad u = 0 \text{ and } \theta \to \theta_0, \tag{13}$$

where θ_0 is the limiting value of the mid-core temperature profile, equation (9) as $y \to 0$. The solution to equation (11) may be written at once, for the lower horizontal boundary layer:

$$\theta = (1 - \mathbf{a})/2 = \theta_b, \tag{14}$$

and similarly, for the upper boundary layer:

$$\theta = (1 + \mathbf{a})/2 = \theta_t. \tag{15}$$

This profile is shown in Fig. 1 and agrees well with the numerically calculated profile, Fig. 2. The constant $\mathbf{a}$ characterizes roughly the temperature difference between the top and bottom horizontal boundary layers in the core. As $Ra \to 0, \mathbf{a} \to 0$ and $Ra \to \infty, \mathbf{a} \to 1$. For a large and finite value of Ra, $\mathbf{a}$ will be close to but still less than one.

The mismatch in $\partial\theta/\partial y$ between equation (9) on one hand and equations (14) and (15) on the other is a measure of the cooling of the top horizontal boundary layer and the heating of the bottom one due to vertical conduction in the core. This heat conduction is very small compared to the heat convection in the boundary layers and has been neglected in this treatment. The numerical simulation of the flow at $B = 5$ and $Ra = 3 \times 10^9$ indicates

$$\int_0^B \left(\frac{\partial\theta}{\partial y}\right)_{y=0.5} \mathrm{d}x \simeq 3.5$$

while

$$\int_0^1 (u\theta)_{x=B/2}\,\mathrm{d}y = 72,$$

thus confirming that the approximation is good.

In calculating the Nusselt number the heat transfer in the stagnant part of the core is neglected. The contribution from the boundary layers is given by

$$Nu = \dot{m}(\theta_t - \theta_b) = \dot{m}\mathbf{a}, \tag{16}$$

where $\dot{m}$ is the dimensionless flow rate in the horizontal boundary layer. To obtain a relation between Nu and Ra-dependent properties of the flow in the core, we begin with the integral form of the momentum equation (10):

$$\frac{1}{Pr}\frac{\mathrm{d}}{\mathrm{d}x}\int_0^\delta u^2\mathrm{d}y = \left(\frac{\partial u}{\partial y}\right)_{y=0} + \frac{1}{2}Ra\cdot\delta^2\cdot\left(\overline{\frac{\partial\theta}{\partial x}}\right), \tag{17}$$

where the bar over $\partial\theta/\partial x$ represents an averaged value across the boundary layer.

Use of any appropriate velocity profile of the form

$$u = C\cdot f(y/\delta) \tag{18}$$

in equation (17) yields the relation:

$$\frac{\mathrm{d}}{\mathrm{d}x}(C^2\delta) = A_1\frac{C}{\delta} + \frac{1}{2}Ra\,\delta^2\left(\overline{\frac{\partial\theta}{\partial x}}\right) \tag{19}$$

where A_1 is a constant independent of Ra and depending only on the shape of the function $f(y/\delta)$, and Pr. For example, use of a velocity profile chosen on the basis of experiment [3], e.g. $u = C\cdot\exp(-y/\delta)\cdot\sin(y/\delta)$, leads to $A_1 = 8\,Pr$.

In the regime under study, the numerical simulations reveal that the horizontal boundary layers in

the core are driven both by the momentum imparted by the vertical boundary layers, and the local buoyancy. The entire regime is therefore characterized by a balance of forces indicated in equation (19) in the core boundary layer. Equating the power dependence of the inertia and friction we obtain from equation (19)

$$C^2\delta \propto C \cdot B/\delta. \tag{20}$$

The $\propto$ sign will be used to denote that both sides of the equation have the same power dependence on Ra. The parallel flow structure in the core (confirmed numerically) implies that the appropriate characteristic scale length in the x direction must be B. Equation (20) thus gives $\delta \propto C^{-1/2}$. This relation together with equation (16) then leads to

$$Nu \propto \dot{m}\mathbf{a} \propto C\delta\mathbf{a} \propto C^{1/2}\mathbf{a}, \tag{21}$$

where from equation (18) the flow rate in the horizontal boundary layer is given by $\dot{m} \propto C\delta$.

4. MATCHING WITH END REGION

For the end region, the following equation may be deduced from Bejan and Tien's [2] equations (32), (36), (39) and (40) and their discussion following their equation (46):

$$Nu = 0.354\, Ra^{1/4}\mathbf{a}^{1/4}. \tag{22}$$

The parameter **a**, representing the temperature differences between the top and bottom horizontal boundary layers in the core, would be an increasing function of Ra, but always less than one. This is confirmed by experiment [3] and by the numerical results. Thus, if the power dependence of Nu on Ra is represented as $Nu \propto Ra^{\mathbf{m}}$, then by equation (22), $\mathbf{m} \geqslant 1/4$.

Equating equations (21) and (22) one obtains:

$$Nu \propto C^{1/2}\mathbf{a} \propto Ra^{1/4}\mathbf{a}^{1/4}, \tag{23}$$

so that

$$C^{1/2} \propto Ra^{1/4}\mathbf{a}^{3/4}. \tag{24}$$

If $\mathbf{a} \propto Ra^{n_1}$ then $n_1 \leqslant 1/3$ since C, the characteristic boundary layer velocity cannot decrease with Ra. This upper limit on power dependence of **a** on Ra, when incorporated into equation (22) yields an upper limit on **m**, $\mathbf{m} \leqslant 1/3$. Further, although **a** increases with Ra, it cannot so increase indefinitely since $\mathbf{a} \leqslant 1$. Therefore, the increase of **a** with Ra must level off and smoothly approach a constant value, probably one, asymptotically as $Ra \to \infty$. This suggests that **m** is not a constant but is rather a decreasing function of Ra and that as $Ra \to \infty$, $Nu \to 0.354\, Ra^{1/4}$ so that

$$Nu_\infty = 0.354\, Ra^{1/4}. \tag{25}$$

The decrease in **m** with increasing Ra within the same flow regime is a reflection of the gradually changing ratio between the buoyant driving forces at the vertical boundary layers on the one hand and the frictional resistance offered by the enclosure on the other, as Ra increases. In other words it reflects the decreasing influence of the core resistance on the vertical boundary layers. Therefore, with the increase of Ra from a low initial value, the transition from the type of flow considered in [2] to the type considered here is characterised by the fact that inertia has just become significant in the core, or by boundary layers of thickness δ lining the horizontal walls with $\delta = O(0.5)$. An order of magnitude examination of equation (19) with $x = O(B)$ then suggests that at this lowest value of Ra within the regime,

$$C^2 = O(4A_1CB),$$

so that $C = O(4A_1B)$ and $\dot{m} = O(2A_1B)$. Using these values in equations (16) and (22) gives us

$$Nu = O(2A_1B)\mathbf{a} = 0.35\, Ra^{1/4}\mathbf{a}^{1/4}.$$

With the value of A_1 obtained in the discussion following equation (19) in the above relation at $Pr = 1$, the following relation between the values of Nu and Ra at the transition from friction-dominated to inertia-dominated flow in the core is given by

$$Nu = O\left(\frac{Ra}{B}\right)^{1/3} 0.1 \tag{26a}$$

i.e.

$$Ra = O(10^3)\, Nu^3 B. \tag{26b}$$

Equation (26) is only an order of magnitude criterion for transition into this high Ra regime and is not intended to represent the power dependence of the heat transfer on Ra, nor on B. Our numerical simulation indicates that transition into the boundary layer regime occurs somewhere between $Ra = 10^6$ and $Ra = 3 \times 10^6$ for $B = 10$ and unit Prandtl number.

From the preceding discussion, it would follow that the dependence of the Nusselt number on the aspect ratio should decrease gradually as the Rayleigh number increases, reflecting the weakening effect of the core-resistance on the vertical boundary layers on the end walls. Asymptotically as $Ra \to \infty$, Nu_∞ from equation (25) is completely independent of B.

The growing independence of Nu from the aspect ratio, B, as the Rayleigh number increases, can also be obtained by the following argument: For a given Ra the influence of B on Nu is through the parameter **a** in equation (22), where $\mathbf{a} = \mathbf{a}(B, Ra)$ (the value of Pr being fixed). For two different values of aspect ratio B_1 and B_2 ($B_1 > B_2$), $\mathbf{a}(B_1, Ra) < \mathbf{a}(B_2, Ra)$. Hence, from equation (22), $Nu(B_1, Ra) < Nu(B_2, Ra)$. But since in the limit $Ra \to \infty$, $\mathbf{a}(B_1, Ra) \simeq \mathbf{a}(B_2, Ra) = 1$, it follows that as $Ra \to \infty$, $Nu(B_1, Ra) \simeq Nu(B_2, Ra)$. Thus the Nusselt number becomes independent of B in the asymptotic limit of $Ra \to \infty$.

In the following analysis, the $\propto$ sign indicates that the expressions on both sides of the $\propto$ sign have the same power dependence on the aspect ratio, B.

The flow rate, $\dot{m}$, in the horizontal boundary layer is given by

$$\dot{m} \propto C\,\delta \propto B/\delta, \tag{27}$$

where we have used equation (20) to eliminate C.

Using this value of $\dot{m}$ in equation (16), and equating this to the power dependence of the Nusselt number on B, through the parameter **a** of equation (22), one gets:

$$Nu \propto B^n \propto \mathbf{a}^{1/4} \propto B\mathbf{a}/\delta. \quad (28)$$

Now, C must be a decreasing function of B, so that shallower enclosures yield lower velocities. Then if the power dependences of δ and **a** on B are expressed as $\delta \propto B^q$ and $\mathbf{a} \propto B^r$, substituting these expressions in equation (27) yields a lower limit on q, $q \geq 1/2$. Substituting for δ and **a** in equation (28) yields:

$$Nu \propto B^{r/4} \propto B^{1+r-q}. \quad (29)$$

Therefore, $n = r/4 = 1 + r - q$, or $r = 4/3\,(q-1)$ and $n = 1/3\,(q-1)$. Thus equation (28) becomes:

$$Nu \propto B^{1/3(q-1)}. \quad (30)$$

At asymptotically high values of Ra, both **a** and Nu are expected to be independent of $B(r \to 0$ and $q \to 1)$. Since Nu should decrease with increasing B, the exponent $(q-1)$ in equation (30) must be negative. This yields an upper limit on q, $q \leqslant 1$. Thus we have $1 \geqslant q \geqslant 1/2$. Substituting this relation in equation (30) gives the relation $0 \geqslant n \geqslant -1/6$, for the power dependence of Nu on B, equation (28). The sensitivity of Nu to B should monotonically decrease with increasing Ra, so that at asymptotically large values of Ra, $q \to 1$, and at lower Ra, we could expect that q is closer to 0.5. This implies from equation (30) that $Nu \propto B^{-1/6}$. Figure 5 illustrates the behavior of n computed from the numerical results for the two aspect ratios ($B = 5$ and 10): n drops monotonically from a value of -0.161 at $Ra = 10^6$ to a value of -0.032 at $Ra = 3 \times 10^9$. This behavior is in good agreement with the prediction.

5. NUMERICAL CALCULATIONS

The flow was numerically simulated by solving the full equations of motion with the Boussinesq approximation. The computer simulation program uses the primitive variables u, v, T and P (pressure) on staggered grids to iteratively solve the full equations of motion. The differencing scheme used in this program proposed by Patankar and Spalding [5] switches between the central difference scheme (CDS) and the upwind difference scheme (UDS) depending on the local grid Peclet number, allowing the retention of numerical stability and giving meaningful numerical results even at the very high Rayleigh numbers investigated here. A grid with variable grid-spacing, with 31 nodes in the y direction and 37 nodes in the x direction was used. The iteration scheme, using the alternating direction implicit (ADI) method, employs extreme under-relaxation in the initial few iterations to ensure numerical stability until an approximate flow pattern is established. The fractional changes in the values of all the field variables at each node from one iteration to the next are monitored. The iterations are terminated when these fractional changes, or residues, fall below a value of 10^{-5}. The execution time for obtaining the numerical solution to the full equations of motion, for flow in an enclosure with $B = 10$ and $Ra = 3 \times 10^8$ was 434 s on the CDC 7600 machine. The numerical code and its validation have been described in detail elsewhere [6, 7].

Results have been obtained with a Prandtl number of unity for two aspect ratios $B = 5$ and 10 for a range of $10^6 \leqslant Ra \leqslant 3 \times 10^9$. The computed temperature profile is shown for the core mid-section in Fig. 2 in agreement with the model, Fig. 1. The horizontal component of the fluid velocity in the core mid-section is shown as a function of vertical distance in Fig. 3. The

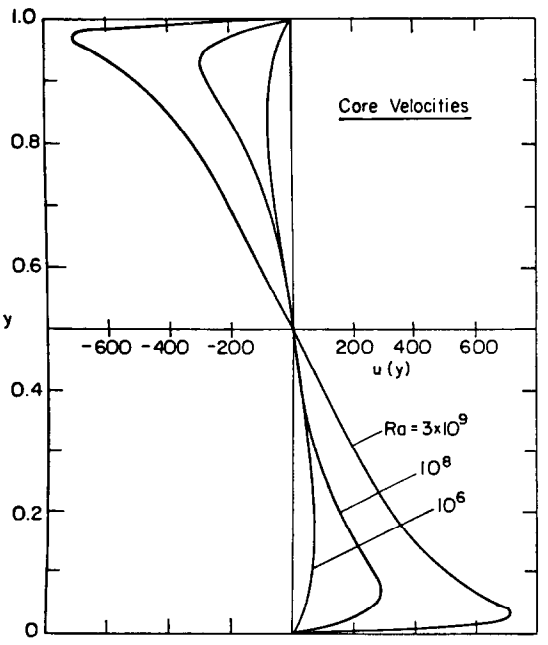

FIG. 3. Computed horizontal velocity distribution in the core, $B = 5$, $Pr = 1$.

qualitative changes in the velocity profile with increasing Rayleigh number are apparent. At $Ra = 10^6$ the velocity profile does not show any boundary layer; at the higher values of Ra, boundary layer structure is evident. The flow profiles do not show the small reverse circulation observed [3]; nor do the boundary layer velocities die off as rapidly towards the center ($y = 0.5$) as in the experiment, so that the center of the core is not quite stagnant but has low velocity fluid within it.

Equation (16), $Nu = \dot{m}\mathbf{a}$, when considered in the light of this numerical result rather than the experiment, would appear to retain its validity, at least approximately. Although it may not now be permissible to assume that the average temperatures in the velocity boundary layers are $(1 + \mathbf{a})/2$ and $(1 - \mathbf{a})/2$ respectively (so that the average temperature difference is no longer **a**), the *difference* in the average temperature between the two thick boundary layers, will be proportional to **a** due to the linearity of the temperature profile away from the walls.

The results from the numerical simulations indicate that buoyancy cannot be neglected in the horizontal boundary layers. For an enclosure with aspect ratio $B = 10$, the value of $(\partial\theta/\partial x)$ in the horizontal boundary layers in the core decreases from 0.010 at $Ra = 10^7$ to 0.008 at $Ra = 10^9$. The isotherms and streamlines in the core are very close to horizontal; the value of $(\partial\theta/\partial x)$ at mid-height ($y = 0.5$) drops from 0.0031 at $Ra = 10^7$, to 0.0017 at $Ra = 10^9$. The size of the core is very close to B. At $Ra = 10^7$, approx. 98% of the enclosure width is occupied by the core, by $Ra = 3 \times 10^9$ this fraction has increased very slightly to about 99% of the enclosure width, thus validating the assumptions and arguments made earlier.

The calculated values of Nu for $B = 5$ and 10 are shown in Fig. 6 together with the experimental results of [3] and the asymptotic prediction according to equation (25). The (local) slope of the log Nu-log Ra curve is the parameter **m** and is shown as a function of Ra in Fig. 4. As predicted by theory, **m** drops continuously from the value of 0.306 at $Ra = 1.7 \times 10^6$ to the value 0.271 at $Ra = 1.7 \times 10^9$ for the case of $B = 5$; and a levelling off at higher Rayleigh numbers is evident from the figure. There is a similar behavior for $B = 10$.

The sensitivity of the Nusselt numbers to B is shown as a function of the Rayleigh number in Fig. 5. As discussed in the previous section, the sensitivity as measured by n, where $Nu \propto B^n$ for a given Ra, should monotonically decrease from some maximum probably close to (but less than) -0.167 towards 0 as $Ra \to \infty$. Figure 5, while being based on only two aspect ratios, clearly exhibits this behavior.

The values of Nu obtained from the numerical simulations could be correlated with Ra according to:

$$Nu = \frac{1}{2^{3/2}} Ra^p, \tag{31}$$

where

$$p = 0.25 - 0.380\, Ra^{-0.1917}, \text{ for } B = 5, \tag{32}$$

and

$$p = 0.25 - 0.472\, Ra^{-0.1917}, \text{ for } B = 10. \tag{33}$$

Equation (32) satisfied all the data points for $10^6 \leqslant Ra \leqslant 3 \times 10^9$ to within 1.7%. Equation (33), for $3 \times 10^6 \leqslant Ra \leqslant 3 \times 10^9$ is accurate to within 1%.

In both these correlations, $p(Ra) \to 0.25$ as $Ra \to \infty$. The importance of distinguishing the variable nature of p from its asymptotic value is illustrated in Fig. 7 where we have plotted the ratio $(Nu_{\text{correlated}}/Nu_{\text{computed}})$ as a function of Ra for the correlation (31, 33) as well as the correlation using the asymptotic value of p, equation (25).

6. COMPARISON WITH EARLIER WORK

There are relatively few published experimental and

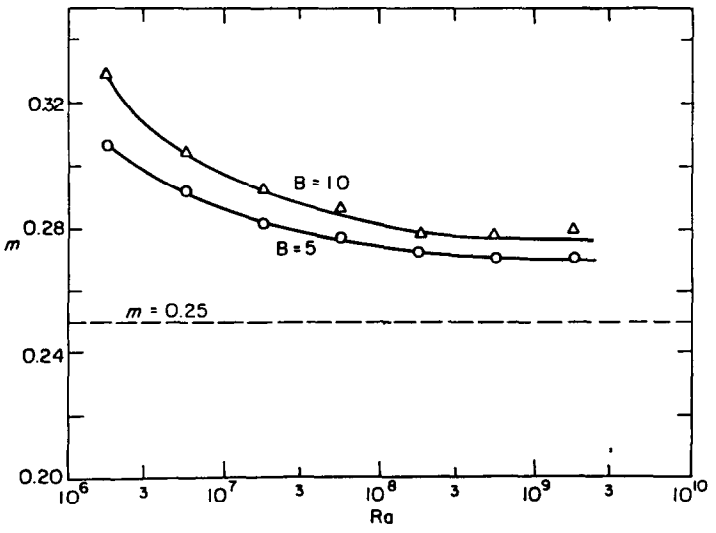

FIG. 4. Rayleigh dependence of **m**, $Pr = 1$, $B = 5$ and $B = 10$.

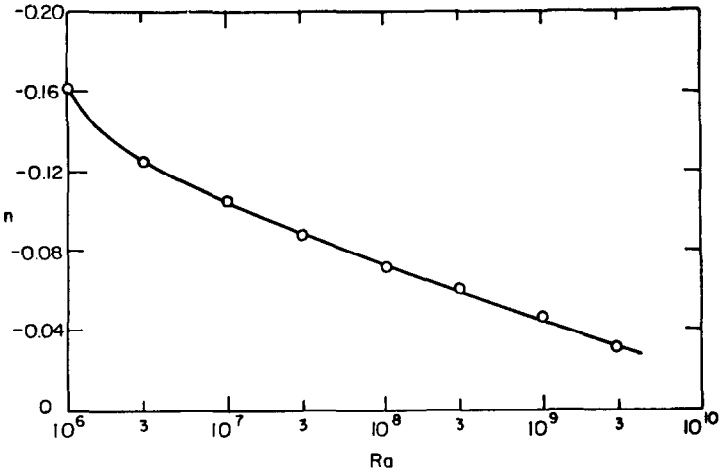

FIG. 5. Computed aspect ratio dependence of Nu between $B = 5$ and $B = 10$ for $Pr = 1$.

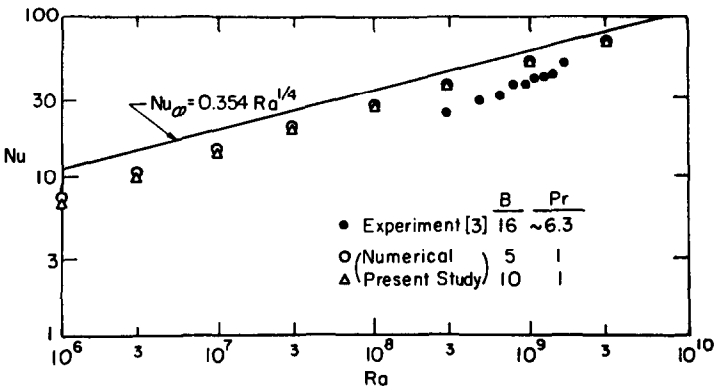

FIG. 6. Heat transfer as a function of Rayleigh number.

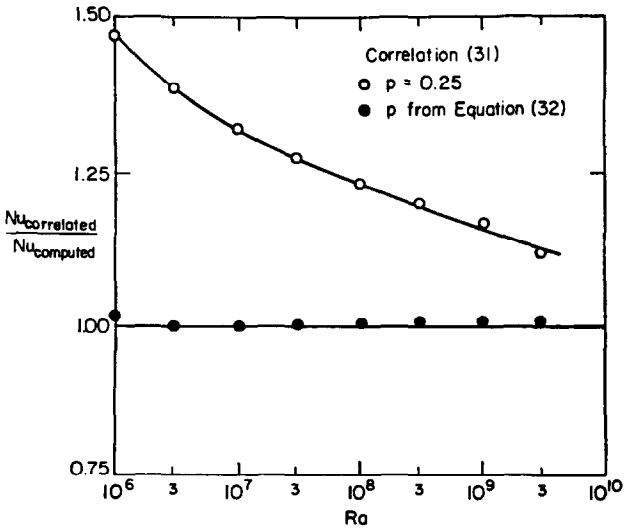

FIG. 7. Ratio of Nu from correlations to numerically computed Nu for $B = 10$, $Pr = 1$.

numerical results for shallow enclosures. However, the limited existing data appear to support the present study. The variation in the exponent **m** in the published correlations presented below could well be a result of different studies having employed straight line fits (to a log Nu–log Ra graph) in different regions of the overall log Nu–log Ra curve. This variation in **m** is between 0.375 and 0.291. Additionally, as the discussion in the previous sections shows, there is good reason for arguing that as $Ra \to \infty$, $\mathbf{m} \to 0.25$.

Al-Homoud and Bejan [3] reported:

$$Nu = (0.0168 \pm 0.0002)\, Ra^{0.375}. \quad (34)$$

It is noteworthy that if their data point for the highest Ra is discarded, their 5 data points located at the higher Ra end of their data exhibit a slope, on a logarithmic plot, close to 0.329. Their data points are shown in Fig. 6. When their data were considered along with those of Imberger [8] they obtained

$$Nu = (0.098 \pm 0.008)\, Ra^{0.291}. \quad (35)$$

The experiments of Imberger [8], when considered independently, appear to support the behavior of the Nusselt number predicted here in the high Rayleigh number regime—witness his Fig. 8, which indicates a change of slope in the log Nu–log Ra curve, approaching 0.25 at the edge of the higher Ra end of the data span.

Tseng's numerical results [9] for $B = 2$, $10^5 \leqslant Ra \leqslant 9 \times 10^7$ show

$$Nu = 0.051\, Ra^{0.329}, \quad (36)$$

while Han's numerical results [10] for $B = 1$, $Pr \geqslant 1$, $Ra = O(10^6)$ give

$$Nu = 0.135\, Ra^{0.313}. \quad (37)$$

7. RELATION TO FLOW IN NARROW VERTICAL ENCLOSURES

In his classical paper on vertical enclosures, Elder [11] reported his experimental observation of the constant thermal stratification in the core for higher Ra, which he was able to explain analytically. His analytical results, based upon his experiments, lead to the following results in our notation:

$$Nu = \mathbf{a} \int_0^{B/2} v(x)\, dx,$$

where **a** is now the stratification in the core in the y direction, and $v(x)$ is the vertical velocity in the core,

$$v(x) \propto Ra^{1/2}\, \mathbf{a}^{-1/2}.$$

The thickness, δ, of the boundary layers lining the vertical walls in the core is given by

$$\delta \propto Ra^{-1/4}\, \mathbf{a}^{-1/4}$$

where the $\propto$ sign denotes Rayleigh dependence. One then obtains:

$$Nu \propto \mathbf{a} v \delta \propto Ra^{1/4}\, \mathbf{a}^{1/4}$$

similar to the shallow enclosure case, equation (22). Elder suggested that **a** is related to the interaction of the two boundary layers lining the vertical walls. His measurements, moreover, clearly indicate that **a**'s power dependence on Ra decreases with increasing Ra and **a** approaches an asymptotic value independent of Ra. These facts, taken together, suggest that in the vertical slot geometry also, the dependence of Nu on Ra cannot be expressed over the whole range of Ra as a simple power law, but that rather the behavior is similar to the shallow enclosure case. The discrepancy in **m** existing in the literature pointed out and discussed by MacGregor and Emery [12] and more recently by Yin *et al.* [13] may well arise from this variation in **m**. A similar situation may account for the discrepancy in n.

8. CONCLUDING REMARKS

The high Ra laminar regime for shallow enclosures has been characterized by its main physical features. The power dependence of the Nusselt number on the Rayleigh number has been predicted according to $Nu \propto Ra^{\mathbf{m}}$. It is indicated that the exponent **m** is a decreasing function of Ra, and not a constant as might otherwise be suspected, decreasing from a maximum probably close to (but less than) 1/3 to a minimum of 1/4 as $Ra \to \infty$. This should be useful not only for understanding this regime, but also as a basis for formulating appropriate Nu correlations. The asymptotic behavior of the Nusselt numbers as $Ra \to \infty$ has been predicted explicitly. The process of $Ra \to \infty$ must be qualified by the probable onset of turbulence before **m** actually reaches 0.25.

The effect of the aspect ratio on the Nusselt number has also been discussed and a correlation has been proposed for the Nusselt number as a function of Rayleigh number based on the results of the numerical simulations. A rough criterion (26) has been proposed, for a given aspect ratio, giving the values of Nu and Ra above which the flow will be characterized by boundary layers lining the horizontal walls in the core.

Acknowledgements—This research was supported by the National Bureau of Standards Center for Fire Research through Grant No. 809253 in part, and in part by the Solar Heating and Cooling Research and Development Branch, Office of Conservation and Solar Applications, U.S. Department of Energy, under contract number W-7405-ENG-48.

REFERENCES

1. D. E. Cormack, L. G. Leal and J. Imberger, Natural convection in a shallow cavity with differentially heated end walls. Part 1. Asymptotic theory, *J. Fluid Mech.* **65**, 209–229 (1974).
2. A. Bejan and C. L. Tien, Laminar natural convection heat transfer in a horizontal cavity with different end temperatures, *J. Heat Transfer* **100**, 641–647 (1978).
3. A. A. Al-Homoud and A. Bejan, Experimental study of high Rayleigh number convection in a horizontal cavity

with different end temperatures, *Report CUMER-79-1*, Department of Mechanical Engineering, University of Colorado, Boulder (1979).
4. A. E. Gill, The boundary layer regime for convection in a rectangular cavity, *J. Fluid Mech.* **26**, 515–536 (1966).
5. S. V. Patankar and D. B. Spalding, Numerical prediction of three-dimensional flows, Imperial College, Department of Mechanical Engineering, Report number EF/T-N/A/46 (June 1972).
6. A. Gadgil, On convective heat transfer in building energy analysis, Ph.D. Thesis, Department of Physics, University of California, Berkeley (1979).
7. F. Bauman, A. Gadgil, R. Kammerud and R. Greif, Buoyancy-driven convection in rectangular enclosures: experimental results and numerical calculations, Paper 80-HT-66, ASME/AICHE National Heat Transfer Conference, Orlando, Florida, July 27–30, 1980.
8. J. Imberger, Natural convection in a shallow cavity with differentially heated end walls. Part 3. Experimental results, *J. Fluid Mech.* **65**, 247–260 (1974).
9. Wen-Fa Tseng, Numerical experiments on free convection in a tilted rectangular enclosure of aspect ratio 0.5, Master's Thesis, Clarkson College (1979).
10. J. T. Han, A computational method to solve nonlinear clliptic equations for natural convection in enclosures, *Numerical Heat Transfer* **2**, 165–175 (1979).
11. J. W. Elder, Laminar free convection in a vertical slot, *J. Fluid Mech.* **23**, 77–98 (1965).
12. R. K. MacGregor and E. F. Emery, Free convection through vertical plane layers—moderate and high Prandtl number fluids, *J. Heat Transfer* **91**, 391–403 (1969).
13. S. H. Yin, T. Y. Wung and K. Chen, Natural convection in an air layer enclosed within rectangular cavities, *Int. J. Heat Mass Transfer* **21**, 307–315 (1978).

CONVECTION A GRAND NOMBRE DE RAYLEIGH DANS DES ENCEINTES ETROITES AVEC DIFFERENTES TEMPERATURES AUX EXTREMITES

Résumé—La convection naturelle laminaire dans des cavités étroites et horizontales (longueur/hauteur $\gg$ 1), avec des parois horizontales adiabatiques et des parois verticales isothermes mais à températures différentes, a été étudiée pour des nombres de Rayleigh très élevés ($Ra \gg 10^6$). On trouve que ce régime d'ecoulement, caractérisé par des couches limites sur toutes les parois, diffère qualitativement du régime à faible Ra, par le fait que les couches limites horizontales sont absentes. L'influence décroissante de Ra sur le nombre de Nusselt et l'effet du rapport de forme sont analytiquement décelés et numériquement verifiés. Une comparaison est faite avec les données expérimentales et numérique, et une nouvelle formule est proposée pour le nombre de Nusselt. Une explication est avancée à propos de la controverse relative à la dépendance du nombre de Nusselt vis-à-vis de Ra dans les espaces étroits verticaux.

FREIE KONVEKTION BEI HOHER RAYLEIGH–ZAHL IN FLACHEN HOHLRÄUMEN MIT UNTERSCHIEDLICHEN ENDTEMPERATUREN

Zusammenfassung—Es wurde für sehr hohe Rayleigh–Zahlen ($Ra \gg 10^6$) die durch Auftrieb bedingte laminare Konvektion in flachen horizontalen Hohlräumen (Breite/Höhe $\gg$ 1) mit adiabaten horizontalen Wänden und isothermen vertikalen Wänden von unterschiedlicher Temperatur untersucht. Es wurde festgestellt, daß dieser Strömungszustand, der durch sowohl an den vertikalen wie an den horizontalen Wänden anliegende Grenzschichten gekennzeichnet ist, sich qualitativ von dem Strömungszustand bei niedrigen Rayleigh–Zahlen unterscheidet, bei dem die horizontalen Grenzschichten fehlen. Der abnehmende Einfluß von Ra auf die Nusselt–Zahl und die Auswirkung des Seitenverhältnisses werden analytisch begründet und dann numerisch bestätigt. Es wird ein Vergleich mit vorhandenen experimentellen und numerischen Daten durchgeführt und eine neue Korrelation für die Nusselt–Zahl bei diesem Strömungszustand vorgeschlagen. Außerdem wird eine Erklärung vorgeschlagen, die auf die gegenwärtige Kontroverse um die Potenzabhängigkeit der Nusselt–Zahl von Ra bei engen vertikalen Kanälen Bezug nimmt.

КОНВЕКЦИЯ В НЕГЛУБОКИХ ПОЛОСТЯХ С ВЕРТИКАЛЬНЫМИ СТЕНКАМИ РАЗЛИЧНОЙ ТЕМПЕРАТУРЫ ПРИ БОЛЬШИХ ЗНАЧЕНИЯХ ЧИСЛА РЕЛЕЯ

Аннотация — Вызванная подъемными силами ламинарная конвекция в неглубоких горизонтальных полостях (отношение ширины полости к длине $\gg$ 1) с адиабатическими горизонтальными и изотермическими вертикальными стенками, имеющими разную температуру, исследовалась при очень больших значениях числа Релея ($Ra \gg 10^6$). Показано, что данный режим течения, характеризующийся наличием пограничных слоев как на вертикальных, так и горизонтальных стенках, качественно отличается от режима течения с малым числом Релея, когда пограничные слои на горизонтальных стенках отсутствуют. Ослабевающее влияние числа Ra на критерий Нуссельта, а также влияние отношения сторон анализируются теоретически и рассчитываются численно. Проведено сравнение с имеющимися экспериментальными и численными данными и предложено новое соотношение для критерия Нуссельта при таком режиме течения. Также предложено объяснение вызывающей обсуждение степенной зависимости числа Нуссельта от Ra в узких вертикальных каналах.